PSEUDO-DYNAMIC SUBSTRUCTURING HYBRID TEST ON FLEXIBLE FRAMES

ZAVALA Carlos[1] OHI Kenichi[2]

TAKANASHI Koichi[3] SHIMAWAKI Yosuke[4]

1.- INTRODUCTION :

In the simulation of the earthquake response of high rise or middle rise buildings, the widely used pseudo-dynamic full-scale on-line test involves the use of large-scale laboratories with the requirement of substantial investment. To reduce it, an advantageous alternative is the use of portions of the structure named sub-structures to be tested, which can reproduce the behavior of the whole structural system in combination with adequate analytical models.

The conventional on-line test[1] assumes an structural system of the type, strong-beam weak-column (shear model), where all the degrees of freedom to be computed are related with the lateral displacements. If a flexible beam-column structural system is considered, complementary degrees of freedom on the structure will appear, and the generation of unbalance forces between steps of integration involves the use of the stiffness of the structural system to compute the complementary displacements. Since the stiffness of the substructure specimen is unknown, analytical predictor must be used to estimate the incremental forces which are produced on the specimen between steps to get the equilibrium of the whole system.

In this paper the removal of the unbalance forces related with the mentioned complementary degree of freedom is presented. Four different predictors of the specimen response, Elastic model, two-component Bilinear model , Multi-Spring model, and Neural Network model[4], are evaluated in order to eliminate and reduce the unbalance forces under constant axial load.
A controlled variation of the moment gradient are considered for the first time in this kind of simulation. Box-shaped sections 100x100x6 are considered as test specimen for the special conditions of the test setup and the required transformations are presented.

2.- HYBRID ANALYSIS :

The mix of experiment and analysis both carried out in parallel, is termed "Hybrid Analysis". If the sub-structuring criterion is applied, one part of our structural system will be tested and the remaining part must follow some analytical model to simulate the response of the whole system. Let's consider that our system to be tested as an hybrid system is a T type structure (Fig.#1); at first our system must be divided into two parts: the specimen and the analytical model. For the test purpose the column has been chosen as the specimen and the left and right hand side beams will be considered as an analytical model. For flexible structural systems under earthquake excitation, the degree of freedom involved in the solution of the problem are the ones shown in Fig.#1. According to these displacements, an incremental analysis must be performed to reproduce the nonlinear characteristics of the system.

In order to carry out the incremental analysis, an stiffness matrix, force vector and displacement vector could be built by the use of an special configuration[2], which considers the degree of freedom associated with mass excitation and the complementary degree of freedom(Fig.#1).

(1) Graduate student, University of Tokyo.
(2) Associate Professor, Institute of Industrial Science, University of Tokyo.
(3) Professor, dittos.
(4) Technical Associate, dittos.

For an earthquake excitation the response on the degree of freedom associated with mass can be computed by solving the dynamic equation of motion :

$$[M]\{\ddot{X}\} + \{Fv\} = -[M]\{I\}\ddot{Y}g \quad .....(1)$$

where [M] : Mass matrix of the structural system.
[Fv] : Force vector associated with mass excitation.

Using the central difference method as integration scheme, the incremental solution for the equation of motion is given by :

$$\{\Delta X\}^{i->i+1} = \{\Delta X\}^{i-1->i} - (\Delta t^2)\{[M]^{-1}\{Fv^i\} + \{I\}\ddot{Y}g\} \quad .....(2)$$

By the use of a condensation of the whole system stiffness matrix, the corresponding displacements vector and force vector are given by:

$$\begin{Bmatrix} \Delta Fv^{i->i+1} \\ \Delta\Omega^{i->i+1} \end{Bmatrix} = \begin{bmatrix} K_{fd} & K_{fo} \\ K_{md} & K_{mo} \end{bmatrix} \begin{Bmatrix} \Delta X^{i->i+1} \\ \Delta\Theta^{i->i+1} \end{Bmatrix} \quad .....(3)$$

At the i-th step, there exist some amounts of unbalance forces denoted by $\{\Delta\Omega^{0->i}\}$, which are caused by material and geometrical non-linearity in the preceding steps :

$$\text{Unbalance force } \{\Delta\Omega^{0->i}\} = \Omega^i - \Omega^0 \quad .....(4)$$

To remove this unbalance between i and i+1 steps, the following is required :

$$\{\Delta\Omega^{i->i+1}\} = -\{\Delta\Omega^{0->i}\} \quad .....(5)$$

When we know the stiffness terms in eq.(3), the scheme of unbalance force removal can be obtained by substituting eq.(5) into eq.(3)

$$\Delta\Theta^{i->i+1} = -[K_{mo}]^{-1}\{\Delta\Omega^{0->i} - K_{md}\Delta X^{i->i+1}\} \quad .....(6)$$

where $\Delta\Omega^{o->i} = \Omega^i - \Omega^o$ is considered to remove the unbalance force.

In the procedure mentioned above, the stiffness matrix of the test specimen must be measured or assumed from the test behavior, to solve the mentioned equation. As is mentioned on reference[3], condensed coordinate transformation and test coordinates (actuator coordinates) transformation are required, and the key of the process is the solution of these displacements($\Delta\Theta^{i->i+1}$).

3.- HYBRID SUBSTRUCTURING SIMULATION

To avoid the difficult task of the stiffness evaluation on the test specimen from the on-line results, a new procedure is presented for the execution of the substructuring hybrid test, using a predictor of the unknown resistance generated in the unbalance between steps. If an Hybrid Simulation is performed, the stiffness of the specimen must be separated from the whole system stiffness matrix to solve the problem.

$\{\Delta\Omega^{i->i+1}\}$ can be divided into two parts; one is contributed by the specimen and the other by the remaining analytical part :

$$\{\Delta\Omega^{i->i+1}\} = \{\Delta\Omega^{*\,i->i+1}\} + \{\Delta\Omega^{S\,i->i+1}\} \quad .....(7)$$

As for the analytical part, stiffness matrices are easily evaluated :

$$\{\Delta\Omega^{*\,i->i+1}\} = [\,K_{mo}^{*}\,]\,\{\Delta\Theta^{i->i+1}\} + [\,K_{md}^{*}\,]\,\{\Delta X^{i->i+1}\} \quad .....(8)$$

where $[\ ^{*}]$ denotes the stiffness matrix without contribution of the specimen.

By substituting eqs.(7) and (8) into eq.(5), we obtain the following scheme, without specimen's stiffness :

$$\{\Delta\Theta^{i->i+1}\} = -\,[\,K_{mo}^{*}\,]^{-1}\,\{\,\{\Delta\Omega^{0->i}\} + \{\Delta\Omega\}^{s\,i->i+1} + [K_{md}^{*}]\{\Delta X^{i->i+1}\}\,\} \quad .....(9)$$

Where $\{\Delta\Omega^{S\,i->i+1}\}$ is the resistance increment of the specimen about non-mass associated degree of freedom.

The uses of a predictor for the evaluation of $\{\Delta\Omega^{S\,i->i+1}\}$ improve the test procedure and avoid the difficult task of the stiffness evaluation on the test specimen, for the removal of the unbalance forces.

4.- PREDICTORS FOR NONLINEAR BEHAVIOR

The performance of four predictors will be evaluated for the solution of the hybrid substructuring response, in order to find the displacements related with minimum unbalance forces.

4.1 Complete Elastic Element Predictor.

In the incremental analysis the stiffness matrix is considered elastic between steps of integration and remaining the same during the execution of all the test. If a condensed coordinate system(Fig.#2) is used, the incremental forces can be computed by :

$$\begin{Bmatrix}\Delta Mi\\ \Delta Mj\end{Bmatrix} = \begin{bmatrix}K_{11} & K_{12}\\ K_{21} & K_{22}\end{bmatrix}\begin{Bmatrix}\Delta\Theta i\\ \Delta\Theta j\end{Bmatrix} \quad ....(10)$$

where

$$K_{11} = K_{22} = 4EI/L$$
$$K_{12} = K_{21} = 2EI/L$$

The advantage in the use of this predictor is the simplicity for the estimation of the forces, that also it takes small time-consuming during the test execution.

4.2 – Two Component Bilinear Elasto Plastic Element Predictor

To predict the unbalance forces, a tangent stiffness matrix for two-component bilinear element[5] is adopted. Considering that each end could produce a work hardening inelastic behavior, the nonlinear effects are simulated. The stiffness matrix is divided into two components, linear and elasto-plastic ones. The stiffness of the linear component remains constant during all the process, but the nonlinear component will take different forms according to the yielding state of the ends. The computation of the moments depends on the state of nonlinearity of the element and the yielding capacity of it. According to this fact, four yielding states are possible for a beam-column element, to produce the change on the nonlinear component :

State A : Linear at i and j

$$\begin{Bmatrix}\Delta Mi\\ \Delta Mj\end{Bmatrix}=\begin{bmatrix}0.2\,EI/L & 0.1\,EI/L\\ 0.1\,EI/L & 0.2\,EI/L\end{bmatrix}\begin{Bmatrix}\Delta\Theta i\\ \Delta\Theta j\end{Bmatrix}+\begin{bmatrix}3.8\,EI/L & 1.9\,EI/L\\ 1.9\,EI/L & 3.8\,EI/L\end{bmatrix}\begin{Bmatrix}\Delta\Theta i\\ \Delta\Theta j\end{Bmatrix} \quad ....(11a)$$

State B : Nonlinear at i and Linear at j

$$\begin{Bmatrix}\Delta Mi\\ \Delta Mj\end{Bmatrix}=\begin{bmatrix}0.2\,EI/L & 0.1\,EI/L\\ 0.1\,EI/L & 0.2\,EI/L\end{bmatrix}\begin{Bmatrix}\Delta\Theta i\\ \Delta\Theta j\end{Bmatrix}+\begin{bmatrix}0.00 & 0.00\\ 0.00 & 2.85\,EI/L\end{bmatrix}\begin{Bmatrix}\Delta\Theta i\\ \Delta\Theta j\end{Bmatrix} \quad ....(11b)$$

State C : Linear at i and Nonlinear at j

$$\begin{Bmatrix}\Delta Mi\\ \Delta Mj\end{Bmatrix}=\begin{bmatrix}0.2\,EI/L & 0.1\,EI/L\\ 0.1\,EI/L & 0.2\,EI/L\end{bmatrix}\begin{Bmatrix}\Delta\Theta i\\ \Delta\Theta j\end{Bmatrix}+\begin{bmatrix}2.85\,EI/L & 0.00\\ 0.00 & 0.00\end{bmatrix}\begin{Bmatrix}\Delta\Theta i\\ \Delta\Theta j\end{Bmatrix} \quad ....(11c)$$

State D : Nonlinear at i and j

$$\begin{Bmatrix}\Delta Mi\\ \Delta Mj\end{Bmatrix}=\begin{bmatrix}0.2\,EI/L & 0.1\,EI/L\\ 0.1\,EI/L & 0.2\,EI/L\end{bmatrix}\begin{Bmatrix}\Delta\Theta i\\ \Delta\Theta j\end{Bmatrix}+\begin{bmatrix}0.00 & 0.00\\ 0.00 & 0.00\end{bmatrix}\begin{Bmatrix}\Delta\Theta i\\ \Delta\Theta j\end{Bmatrix} \quad ....(11d)$$

4.3 Multi-spring Element Predictor

Another kind and more accurate model for the prediction of the incremental forces is a multi spring joint model[6]. For this model the beam-column element is divided into two portions (Fig.#3a): one is an elastic beam member and the others are multi-spring inelastic joints. The length of the multi-spring joint(l) is assumed to be constant during the analysis and its appropriate value depends on the size of the inelastic zone anticipated in each problem. The multi spring joint consists of four bar-springs and a shear panel. Each bar-spring is located in parallel at the distance r_n from the central axis and connected to both ends of the joint. Each spring will carry axial load and will follow an hysteresis rule as is described in reference [6].
If a system coordinate is used the incremental moments at the ends of the joints are defined as :

$$\Delta Mi = r_n K_n (\Delta Xj - \Delta Xi) + 0.5\, l\, K_s (\Delta Yi - \Delta Yj) + (r_n^2 K_n + 0.25\, l^2 K_s)(\Delta\Psi i - \Delta\Psi j) \quad ....(12a)$$

$$\Delta Mj = r_n K_n (\Delta Xi - \Delta Xj) + 0.5\, l\, K_s (\Delta Yj - \Delta Yi) + (r_n^2 K_n + 0.25\, l^2 K_s)(\Delta\Psi j - \Delta\Psi i) \quad ....(12b)$$

where K_n is the tangent stiffness of the spring n and ΔXi, ΔYi, $\Delta\Psi i$,ΔXj, ΔYj, $\Delta\Psi j$ are the incremental deformations on the degree of freedom expressed in member coordinate.

4.4 Artificial Neural Network Predictor

The use of a Neural Network is a new procedure for the execution of the substructuring hybrid test. Here we use a neural network based on the multi-layer back propagation error learning algorithm[10].
As is named, artificial neural network is analogous to artificial brain which is trained for a specific purpose, in our case to predict the incremental forces; the neural network requires an input vector to be activated and provides an output, which is identical or close to the desired training data. The training is a systematic process to modify the parameters of the neural network in order to achieve the training data through the sampling presentation of these to the network. In this way our artificial brain learns to associate the input vector with the desired output and create a complex nonlinearity by itself.

The advantage of Neural Network over other type of predictor (Prescribed analytical model) is due to the capacity of self-organizing and learning of the network. For that, training prior to the test of the network is required, which is performed using previous test responses or calibration test; the reason is due to the high demand of time in the learning process, which sometimes takes hours or even days[8].

If the reader is not familiar with neural networks, we recommend reference [7] and [8] for the general knowledge of the problem. References [4] and [9] treat specific examples related with the implementation of the neural network model in the hybrid test.

An implementation of the back propagation algorithm is developed on ZOT, a neural network simulator coded in fortran by the authors. The simulator was installed on a Sun Sparc-10 Workstation in order to achieve the training process with the supervision of the operator and carried out the experimentation and improvement of the parameters of the network.

For 300 sets of data, which are the results of previous response tests with varying moment capacity in both ends (ΔMi and ΔMj) and axial capacity (ΔN), ZOT performs the training of the network. The neural network considered in this case has three layer(Fig.#3b); the number of input units was 21. A hidden layer with 42 unit and an output layer with 3 units (ΔMi,Δ Mj,Δ N), are adopted. For these cases the rate value for the modification of the gradient was equal to 0.000065 at the beginning of the process. Each set of data was composed of six original data ($\Delta\theta$i,ΔMi,$\Delta\theta$j,ΔMj,$\Delta\delta$,ΔN) which generate the following input data:

1 – Actual angle increment ($\Delta\theta i^{k}$)
2 – Previous Moment increment (ΔMi^{k-1})
3 – Minimum angle increment till step k ($\Delta\theta i^{min<k}$)
4 – Moment increment for the minimum angle increment ($\Delta Mi(\Delta\theta i^{min<k})$)
5 – Maximum incremental angle till step k ($\Delta\theta i^{max<k}$)
6 – Moment increment for the maximum angle increment ($\Delta Mi(\Delta\theta i^{max<k})$)
7 – Angle increment at last turning point of angle velocity ($\Delta\theta i^{trn}$)
8 – Actual angle increment ($\Delta\theta j^{k}$)
9 – Previous Moment increment (ΔMj^{k-1})
10 – Minimum angle increment till step k ($\Delta\theta j^{min<k}$)
11 – Moment for the minimum angle increment ($\Delta Mj(\Delta\theta j^{min<k})$)
12 – Maximum angle increment till step k ($\Delta\theta j^{max<k}$)
13 – Moment increment for the maximum angle increment ($\Delta Mj(\Delta\theta j^{max<k})$)
14 – Angle increment at last turning point of angle velocity ($\Delta\theta j^{trn}$)
15 – Actual normal displacement increment ($\Delta\delta^{k}$)
16 – Previous Normal Force increment (N^{k-1})
17 – Minimum displacement increment till step k ($\Delta\delta^{min<k}$)
18 – Force increment for the minimum displacement increment ($\Delta N(\Delta\delta^{min<k})$)

19 – Maximum displacement increment till step k ($\Delta\delta^{max<k}$)
20 – Force increment for the maximum displacement increment ($\Delta N(\Delta\delta^{max<k})$)
21 – Normal displacement increment at last turning point of deformation velocity ($\Delta\delta^{trn}$)

After 60000 sweeps of presentation for the 300 data the training data were reproduced with enough accuracy .

5– TEST PROCEDURE

In the execution of an hybrid simulation, three coordinate systems must be assumed in order to perform the analysis, reproduce the displacement configuration of the beam–column specimen and drive the actuator system to reach the desired deformed position for the measure of the restoring forces involved in the simulation. For the T structure, the column has been adopted as test specimen, where the top(j=B) is connected with analytical parts where unbalance forces are generated, and the bottom(i=A) is a fixed end. At first, the member coordinates of the element are shown in Fig.#1. Let's condense this member coordinate of six degree of freedom and turn it into a three degree of freedom condensed coordinate system as is shown in Fig.#2, where the forces related with this condensed coordinate system are the end moments and the normal force, and the convention of positive sign is also presented. These systems are related through a transformation[4] of the following type:

$$[P]=[C]\{M\}=\begin{Bmatrix} Pxi \\ Pyi \\ Mi \\ Pxj \\ Pyj \\ Mj \end{Bmatrix}=\begin{bmatrix} 0 & 0 & -1 \\ -1/H & -1/H & 0 \\ 1 & 0 & 0 \\ 0 & 0 & 1 \\ 1/H & 1/H & 0 \\ 0 & 1 & 0 \end{bmatrix}\begin{Bmatrix} Mi \\ Mj \\ N \end{Bmatrix} \qquad \begin{Bmatrix} \Theta_A \\ \Theta_B \\ \delta \end{Bmatrix}=t[C]\begin{Bmatrix} xi \\ yi \\ \psi i \\ xj \\ yj \\ \psi j \end{Bmatrix} \qquad \text{....(13)}$$

By use of the transformation mentioned above, the member coordinates (Fig.#1) and the condensed coordinates (Fig.#2) can be switched to each other; a test setup(Fig.#4 and Photo) with the capacity to reproduce the condensed coordinate configuration was built. Another transformation is required to relate the condensed coordinate displacements with the test coordinate displacements, which are used to control the actuator stroke movement. Then following the nomenclature of Fig.#5, the transformations are given by :

$$\begin{Bmatrix} M_A \\ M_B \\ N \end{Bmatrix}=\begin{bmatrix} 0 & -L_1 & 0 \\ \dfrac{-(L_2 L_3)}{(L_2+L_3)} & \dfrac{(L_1 L_3)}{(L_2+L_3)} & 0 \\ 0 & 0 & \dfrac{(L_5+L_6+L_7)}{(L_5+L_6)} \end{bmatrix}\begin{Bmatrix} FF_{(1)} \\ FF_{(2)} \\ FF_{(3)} \end{Bmatrix} \qquad \text{....(14)}$$

$$\begin{Bmatrix} Xex_{(1)} \\ Xex_{(2)} \\ Xex_{(3)} \end{Bmatrix}=\begin{bmatrix} 0 & -\dfrac{(L_3 L_2)}{(L_2+L_3)} & 0 \\ -L_1 & \dfrac{(L_3 L_1)}{(L_2+L_3)} & 0 \\ 0 & 0 & \dfrac{(L_5+L_6)}{(L_5+L_6+L_7)} \end{bmatrix}\begin{Bmatrix} \Theta_A \\ \Theta_B \\ \delta \end{Bmatrix} \qquad \text{....(15)}$$

Where $Xex_{(k)}$ is the stroke displacement in the actuator k and $FF_{(k)}$ is the actuator force in the same actuator. L_k are defined by the test setup configuration on Fig.#5

Due to the sensivity of the axial displacement control(δ), a mixed control for the actuators was used during the test. Actuators 1 and 2 (Fig.#4) were controlled by displacement and actuator 3 was controlled by load, in this way, the axial force N is the command signal and the axial deformation δ is measured directly from the test setup.

For the execution of this test, two personal computers were linked with each other through serial port. One computer was used for the structural analysis of the whole system and the other computer was used for the control of the actuators and the measurement of the specimen responses.

On the structural analysis computer, the procedure start at the step i of integration as follow: the forces on the specimen were measured at the step i. Using the central difference method as integration scheme, the incremental displacements between the step i and i+1 are computed using eq.(2). At this step the prediction of the incremental resistance of the specimen $\{\Delta\Omega^{S\ i->i+1}\}$ is required and eq.(9) is solved. Then the transformation to condensed coordinate displacements (Θ_A, Θ_B) is performed and these values are transferred to the actuator control computer, which executes the transformation from condensed coordinate to test coordinate(actuator system) and command this signal in order to reach the desire target condensed displacements. When the target is reached, the forces on the specimen were measured and the inverse transformation is executed; these values are transferred to the structural analysis computer, where these values update the restoring forces, to continue with the next step of integration.

6-TEST RESULTS

Using the sub-structuring concepts by the use of equations (2) and (9), the hybrid test can be performed with the use of the resistance predictors described above. Taking the T structure as prototype for this simulation, where all the elements are box shapes of 100x100x6, with beam length(Lb1,Lb2) of 150 cm. and the column length(L2) of 130.8 cm.; Dimensions of the test specimens, results of the material test and stub column test are shown in Tables 1, 2, and 3.
The system was subjected to the NS component recorded at El Centro earthquake with duration of 8 seconds and peak acceleration of 250 gals.; for this test the mass was considered equal to 0.0311296 ton.sec^2/cm, under constant axial load of 33 tons. (around 40% of the axial capacity).

For the elastic predictor task, the stiffness matrix considers geometrical non-linearity. In the case of the two-component bilinear model, the update of the stiffness matrix and the non-linearity has been considered, also the moment capacity was calibrated with previous test responses. For the case of the multi-spring model, the parameters of the spring, were calibrated by the use of the material test, stub column test and the previous responses. By the use of the previous responses, the training of the neural network was performed for a set of 300 steps, leaving the network without learning the last 500 steps in order to observe the self-organization of the model.

The evaluation of the moments around the node B and the corresponding unbalance moment around it for each of the predictors were performed. These results of are shown on Fig.#6 and Fig.#7. Fig.#6 shows us that the equilibrium of the node is satisfied for all the predictors, where the left side, right side beam moments and the top specimen moment are in equilibrium almost completely. From Fig.#7 is possible to read that the unbalance has been removed in all the cases. The minimum of unbalance force is provided in the multi-spring predictor case. Also if the time is consider as a decision factor in the choice of the best predictor, a simple and fast alternative

with acceptable accuracy is the use of the bilinear predictor. Table 5 shows the peak value of the unbalance force. The neural network predictor satisfies the self-organizing concept and the unbalance moment is less than 6% of the maximum moment after 300 steps when the training was not performed.

In order to accept the true hybrid response obtained by the simulations, complete numerical analysis with the use of multi-spring model was performed. Results of the moment vs. rotation relations for both ends of the specimen and the shear resistance vs. drift are shown in Fig.#8 and Fig.#9; also the yield moments, maximum moments and shear capacities are shown in Table 4.; Similar results for the maximum shear capacity have been found.

7-CONCLUSIONS

(1) The removal of the unbalance forces is possible and the use of the sub-structuring hybrid system for framed structures provides a powerful tool for the full-scale simulation with low investment and acceptable precision.

(2) Different predictors have been evaluated, where the minimum unbalance after the removal was found on the multi-spring model, but with the longest demand of time; an alternative with acceptable results and low time-consuming is the use of a two component bilinear model for the prediction of the restoring forces.

(3) Controlled variation of the moment gradient has been considered for first time in this kind of simulation by the use of the condensed coordinate system and the associated test-setup configuration created for this purpose; this permits the study of the real behavior under these conditions.

(4) This is the first experience with neural network in on-line hybrid test; from the obtained results is possible to conclude that more accurate training of the artificial neural network is required to decrease the amount of unbalance after the removal; also good self organization for the non-training data and the capacity to reproduce the non-linearity of inelastic beam-columns have been observed.

8-REFERENCES

[1]-Takanashi K. :Seismic Failure Analysis of Structures by Computer-Pulsator On-line System. Journal of IIS.,Vol.26,N.11,1974, University of Tokyo.

[2]-Kanan A. & Powell G.: Drain- 2D User's guide. UCB/EERC,1973, University of Berkley USA.

[3]-Zavala C./ Ohi K./ Chen Y. : Special Factors on Sub-structuring Hybrid Simulation Implementation.1992 Seminar of Kanto Chapter of Architectural Institute of Japan.

[4]-Zavala C./ Ohi K. / Takanashi K.: Neural Network Predictor in Hybrid Earthquake Response Performance and Applicability, 1993 Journal of Structural Engineering Vol.40B, Architectural Institute of Japan.

[5]-Melbourne F. Gilberson: Two Nonlinear Beams with Definitions of Ductility. February 1969. Journal of Structural Division ASCE. USA.

[6]-Ohi K./ Takanashi K. / Meng L. : Multi Spring Joint Model for Inelastic Behavior of Steel Members with Local Buckling, March 1991 Bulletin of ERS. IIS N.24 - University of Tokyo.

[7]-Dan Hammerstrom - Adaptive Solutions Inc. : Neural Networks at Work June 1993, IEEE Spectrum USA.

[8]–Dan Hammerstrom – Adaptive Solutions Inc. : Working with Neural Networks July 1993, IEEE Spectrum USA.

[9]–Zavala C./ Ohi K. / Takanashi K. : Neural Network Model in Substructuring Hybrid Simulation ,1993 Annual Meeting of the Architectural Institute of Japan.

[10]–Rumelhart D./ Hinton G. / Williams R. : Learning Representations by Back Propagation Errors, 1986 Parallel Distributed Processing: Explorations in Microstructures of Cognition, Vol 1. Cambridge, MA; MIT Press pp 318–362.

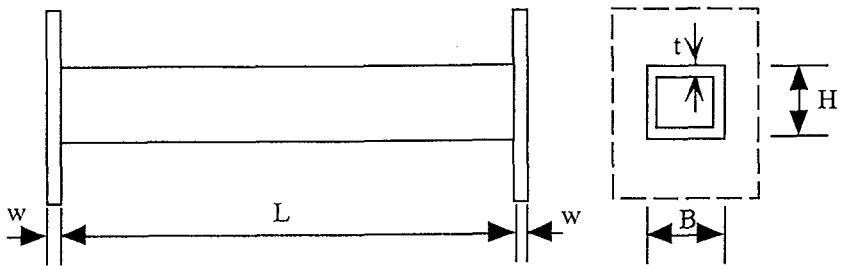

Table 1 . Specimen Dimensions

Test Name	w (cm)	t (cm)	L (cm)	B (cm)	H (cm)	A (cm^2)	I (cm^4)	Predictor used on Test
TEL09	0.30	0.61	127.10	10.096	9.958	22.625	337.294	Elastic
TBI06	0.30	0.61	127.00	10.064	9.968	22.598	337.247	Bilinear
TMS07	0.30	0.61	127.00	10.077	9.985	22.634	338.971	Multi–spring
TNE02	0.30	0.61	127.10	10.080	9.976	22.979	338.323	Neural Network

Table 2 : Results of the Material Test

TEST	B	t	A	L	Py	Pu	σy	σu	Est/E	σy/σu	δb	δb/L
	cm	cm	cm^2	cm	ton	ton	ton/cm^2	ton/cm^2			cm	
T1	4.00	0.605	2.42	20.0	8.77	11.06	3.625	4.570	1/98	79.3	5.1	25
T2	4.00	0.610	2.44	20.0	8.87	11.08	3.637	4.541	1/90	80.1	5.4	27
T3	4.00	0.610	2.44	20.0	8.08	10.82	3.312	4.434	1/77	74.7	5.4	27
T4	4.00	0.610	2.44	20.0	8.84	11.00	3.625	4.508	1/87	80.4	5.1	25
T5	4.00	0.605	2.42	20.0	8.69	10.94	3.594	4.521	--	79.5	5.2	26

Table 3 :RESULTS OF THE STUB TEST

Stub	B	t	A	L	Py	Pu	σy	σu	σy/σu
	cm	cm	cm^2	cm	ton	ton	ton/cm^2	ton/cm^2	
STC1	10.02	0.611	23.73	30.0	83.8	94.6	3.531	3.986	88.6
STC2	10.05	0.613	23.89	30.0	83.6	94.0	3.500	3.935	89.9
STC3	10.03	0.617	23.99	30.0	85.4	95.3	3.562	3.972	89.6

Table 4. : Maximum Values of the Response for T structure Hybrid Test.

Predictor	Specimen	My (ton.cm)	Θy (rad) xE-03	Mmax (ton.cm)	Θmax (rad) xE-02	Qy (ton.)	Xy (cm.)	Qmax (ton.)	Xmax (cm.)
Elastic	TEL09	237.06	6.842	338.91	5.372	3.302	2.126	4.635	8.477
Bilinear	TBI06	241.37	8.082	351.03	8.329	3.203	1.895	4.754	11.244
Multi-spring	TMS07	245.68	7.714	341.66	3.977	3.114	1.624	4.338	6.642
Neural Network	TNE02	246.48	14.91	353.59	8.925	3.170	1.920	4.506	11.717

Table 5. : Remain Unbalance after the remove in percent of the maximum Moment for 8 sec. of El Centro Earthquake

Predictor	Specimen	Unbalance (%)	Test execution time (min.)
Elastic	TEL09	14.506	171
Bilinear	TBI06	11.258	158
Multi-spring	TMS07	6.377	199
Neural Network	TNE02	13.160	204

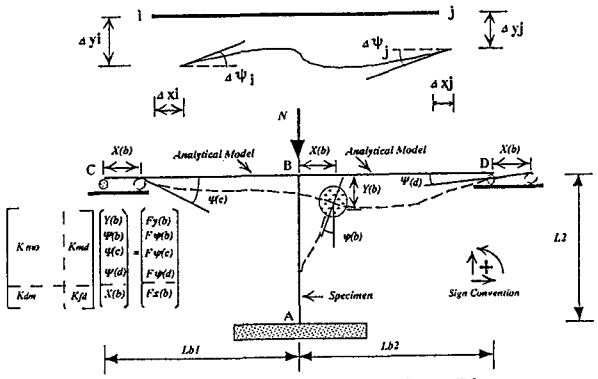

Fig. # 1 : System Coordinate and Degree of freedom on T Stucture

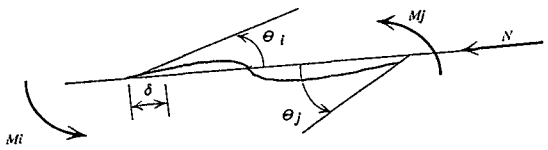

Fig. # 2 Condensed Coordinate System

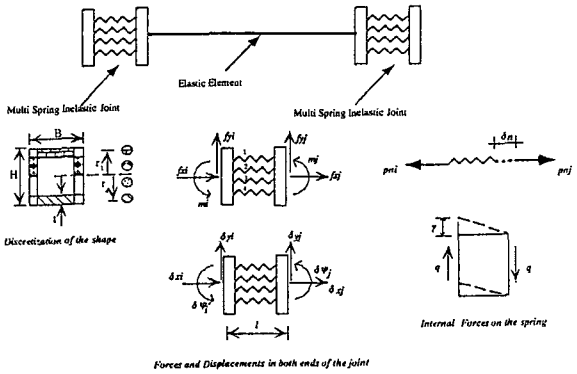

Fig. # 3a : Multi spring joint element

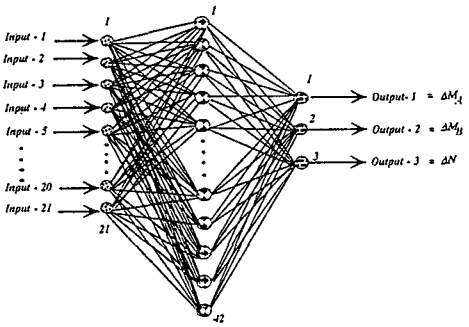

Fig. # 3b : Neural Network Topology

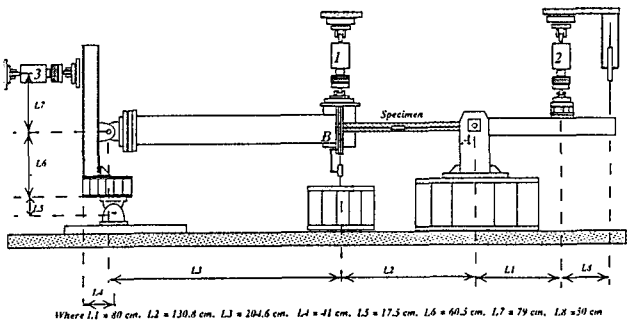

Fig. # 4 : Test Setup for Substructuring Hybrid Test

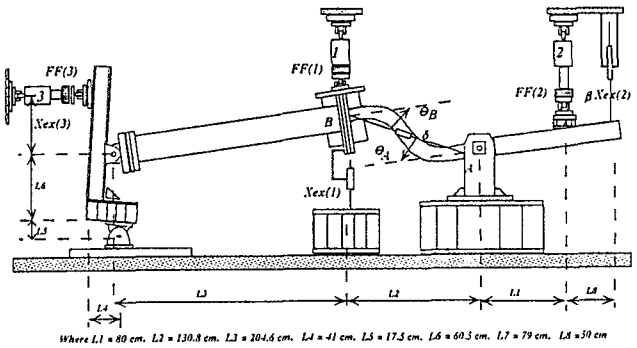

Fig. # 5 : Test Coordinate System and Condensed Coordinate System on the Setup

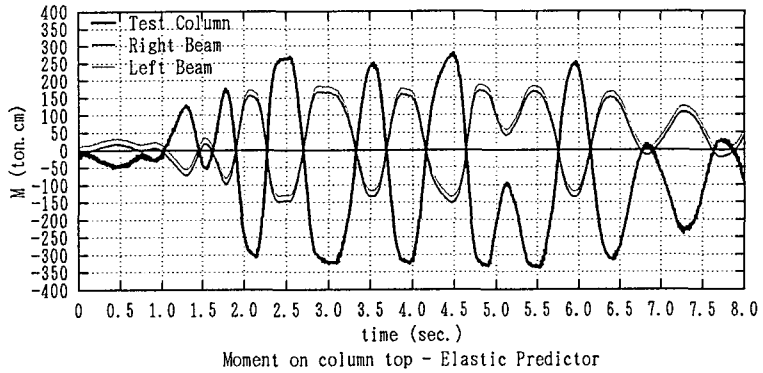

Moment on column top - Elastic Predictor

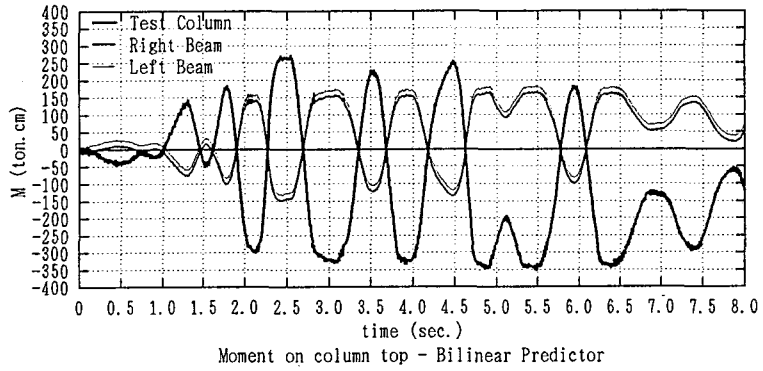

Moment on column top - Bilinear Predictor

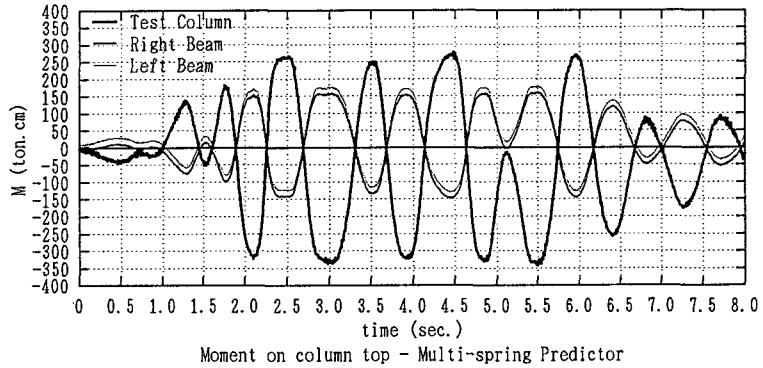

Moment on column top - Multi-spring Predictor

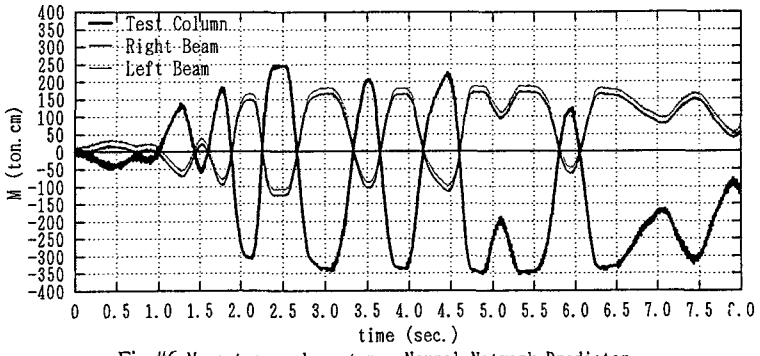

Fig.#6 Moment on column top - Neural Network Predictor

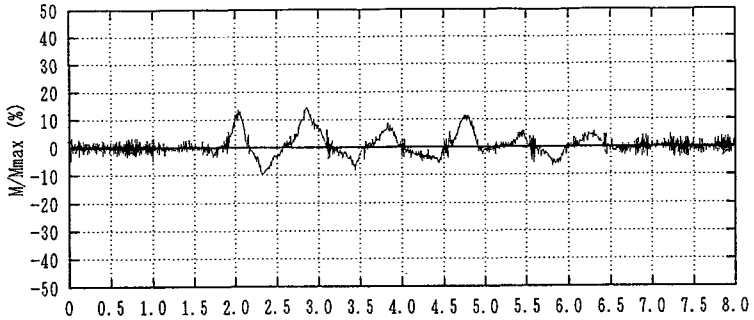

Unbalance Moment column top - Elastic Predictor

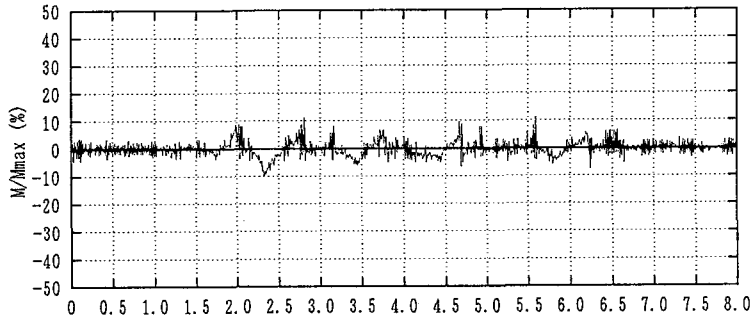

Unbalance Moment column top - Bilinear Predictor

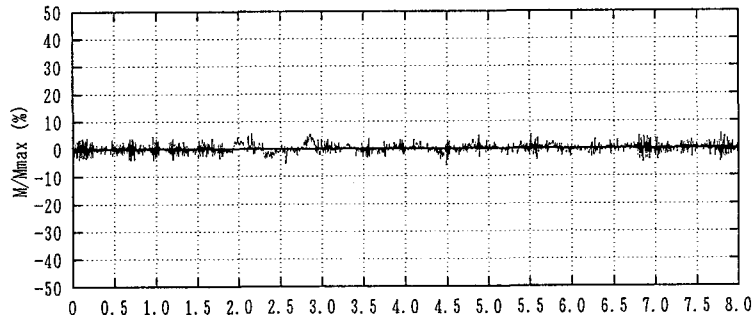

Unbalance Moment column top - Multi-spring Predictor

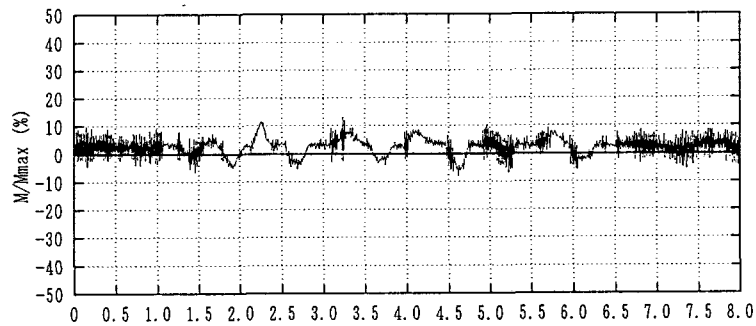

Fig.#7 Unbalance Moment column top - Neural Network Predictor

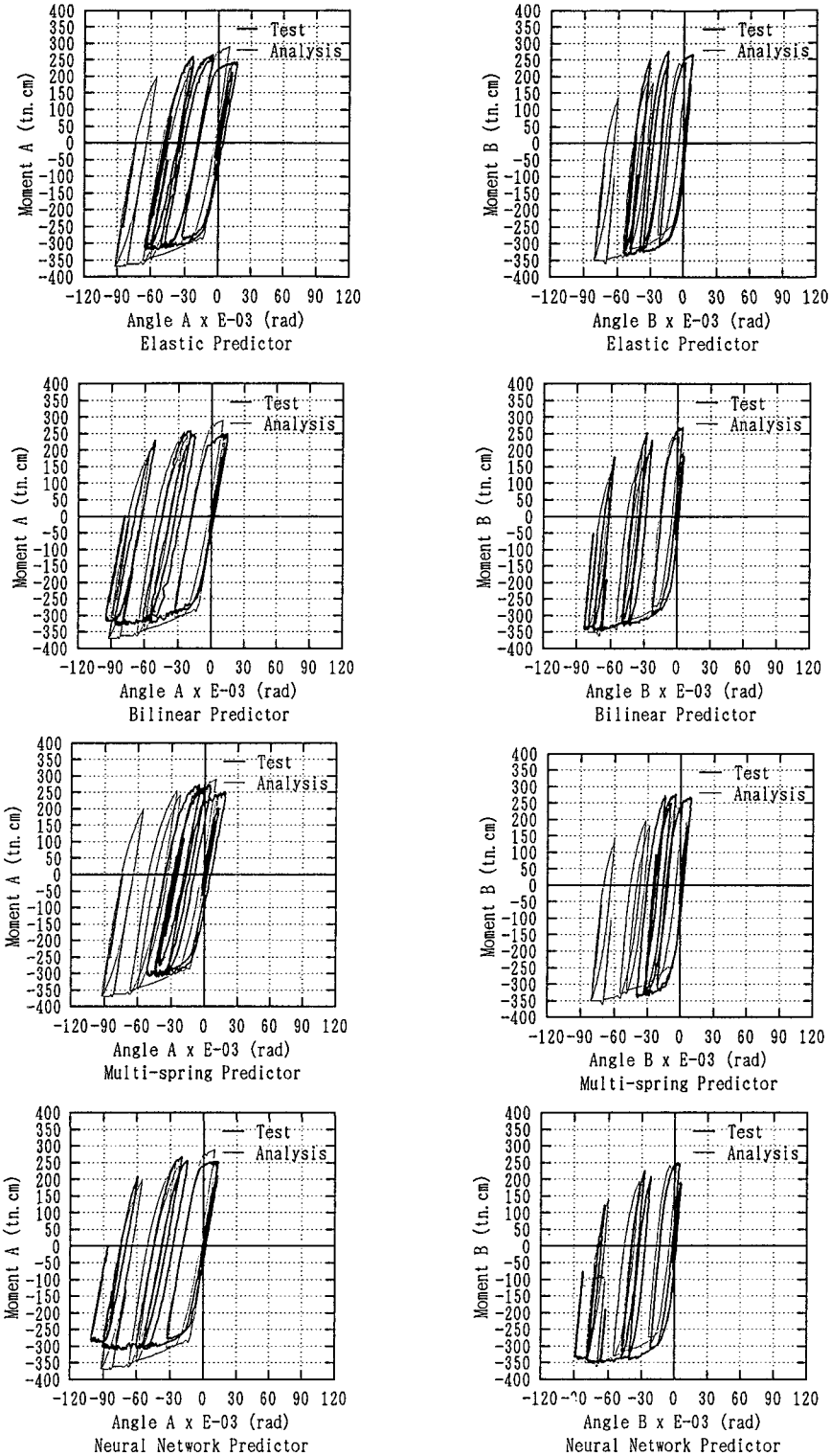

Fig.#8 Moment vs Rotation Relations

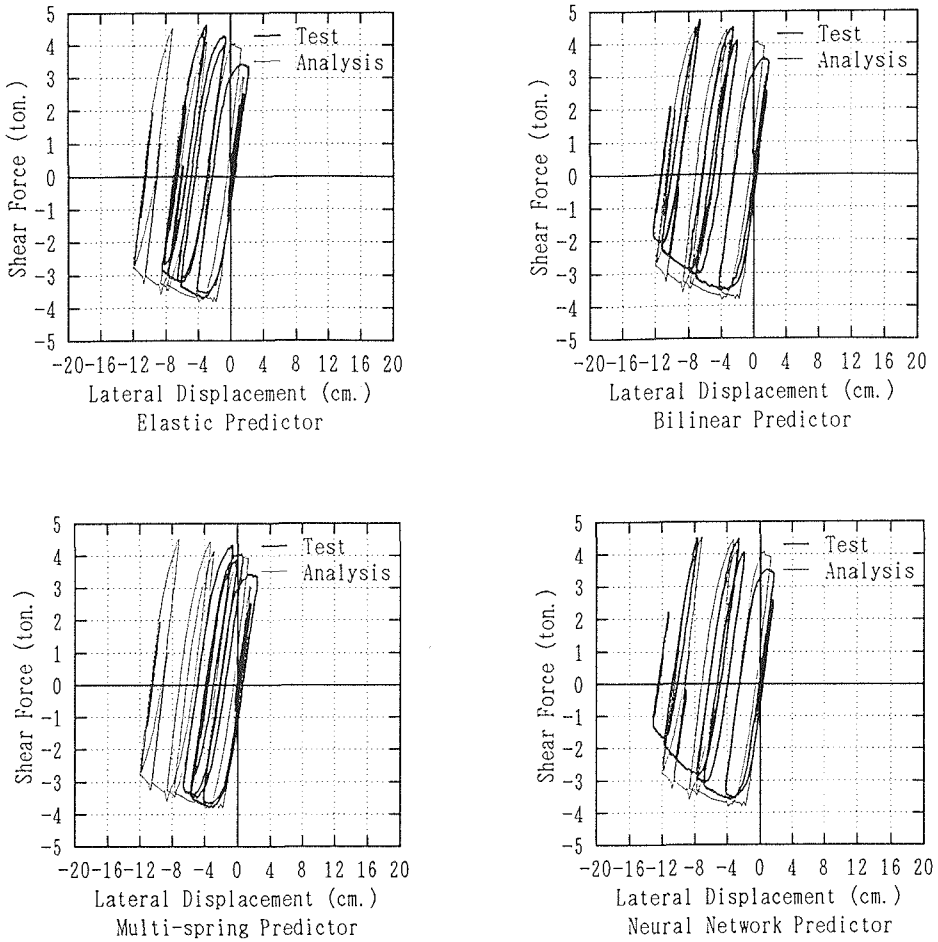

Fig.#9 Shear Resistance vs. Drift Relations

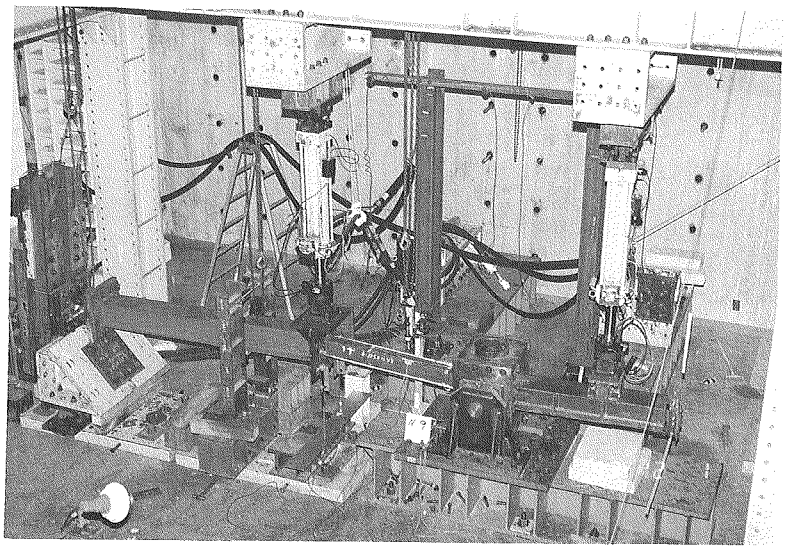

Photo : Test Setup